

Synthesis of CoOOH Nanorods and Application as Coating Materials of Nickel Hydroxide for High Temperature Ni–MH Cells

W. K. Hu,[†] X. P. Gao,^{*,‡} M. M. Geng,[§] Z. X. Gong,[§] and D. Noréus[†]

Department of Structural Chemistry, Arrhenius Laboratory, Stockholm University, S-106 91 Stockholm, Sweden, Institute of New Energy Material Chemistry, Department of Materials Chemistry, Nankai University, Tianjin 300071, China, and Tianjin Peace Bay Power Sources Group Co. Ltd., Tianjin 300384, China

Received: December 2, 2004; In Final Form: February 16, 2005

Studies on nanoscale materials have received great interest in both fundamental and applied aspects in recent years. In this letter, we report the synthesis of CoOOH nanorods and their possible applications as coating materials on nickel hydroxide for high-temperature nickel–metal hydride (Ni–MH) cells. The morphology and structure of CoOOH nanorods and coated nickel hydroxide particles are investigated by transmission electron microscopy, X-ray diffraction, and scanning electron microscopy, respectively. The electrochemical properties in the cylindrical AA size Ni–MH cells are evaluated. Our results show that the Ni–MH cells, where the positive electrodes are composed of such nanometer sized CoOOH coatings, have a higher capacity available and good performance at elevated temperatures of $> 50\text{ }^{\circ}\text{C}$.

Cobalt oxide and hydroxide are important magnetic materials,^{1–3} catalytic materials,^{4–9} ionic exchangers,^{10,11} as well as electrode materials.^{12–19} Cobalt oxide is an indispensable component in the positive electrodes of rechargeable alkaline nickel-based batteries to achieve high electrochemical efficiency. The co-deposition of cobalt hydroxide or addition of cobalt oxide into nickel hydroxide beneficially improves utilization and conductivity of active materials¹³ and increased the charge efficiencies.^{14–19} The surface modification of spherical nickel hydroxide by cobalt was also found to be effective to enhance the reversibility of the β (II) $\text{Ni}(\text{OH})_2/\beta$ (III) NiOOH redox reaction and electrode performance.^{20,21} Whether it is cobalt, cobalt oxide, or cobalt hydroxide, however, they are finally converted into CoOOH on the surface of electrodes after chemical oxidation or electrochemical oxidation in the strong alkaline media.^{14,22} Due to the higher conductivity phase of the formed CoOOH than the NiOOH , the conductive networks among nickel hydroxide particles were considered to be enhanced,¹⁴ leading to improvement of charge efficiency and cycling stability. However, it is very important to make uniform distribution of CoOOH on the surface of nickel hydroxide. Therefore, surface modification of each nickel hydroxide particle using CoOOH is a key issue. Herein, we report the synthesis and characterization of CoOOH nanorods and their applications as direct coatings on the surface of spherical nickel hydroxide particles. The nickel–metal hydride (Ni–MH) cells composed of such nanostructural-coated nickel electrodes were constructed to demonstrate high performance at elevated temperatures of more than $60\text{ }^{\circ}\text{C}$.

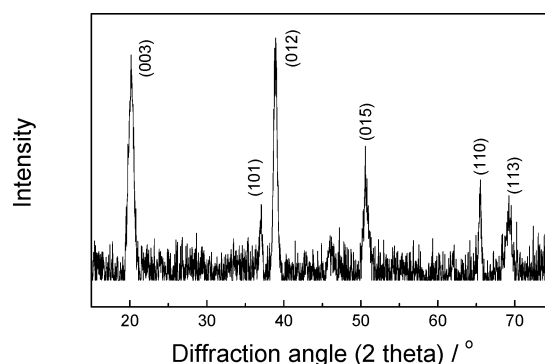


Figure 1. XRD pattern of the CoOOH sample.

The CoOOH nanorods were synthesized by the following processes. A 0.05 M oxalic acid solution was dropped stepwise into a 0.05 M cobalt sulfate solution at $45\text{ }^{\circ}\text{C}$. A pink precipitate was obtained and then filtered, washed with distilled water, and dried at $65\text{ }^{\circ}\text{C}$. The precipitate was dissolved in water under magnetic stirring at $45\text{ }^{\circ}\text{C}$ and a 1.0 M sodium hydroxide solution was dropped. The addition of the sodium hydroxide solution was terminated when the pH value of the solution reached about 10. The precipitate was then moved to a 8 M NaOH solution and subsequently was treated by adding 2–4 mL of a 30% H_2O_2 solution at $60\text{ }^{\circ}\text{C}$, and it remained for 16 h at the same temperature. Finally, the treated precipitate was washed with distilled water to neutral, filtered, and dried at $65\text{ }^{\circ}\text{C}$. The sample obtained was characterized by power X-ray diffraction (XRD) with $\text{Cu K}\alpha 1$ (1.5406 \AA) radiation. Figure 1 shows the XRD pattern of the sample, in which all of the refraction peaks can be indexed to a rhombohedral structure of CoOOH with a space group of $R\bar{3}m$ and a unit cell parameter of $a = 2.8615\text{ \AA}$ and $c = 13.2143\text{ \AA}$. The d spacing at the

* To whom correspondence should be addressed. E-mail: xpgao@nankai.edu.cn.

[†] Stockholm University.

[‡] Nankai University.

[§] Tianjin Peace Bay Power Sources Group Co. Ltd.

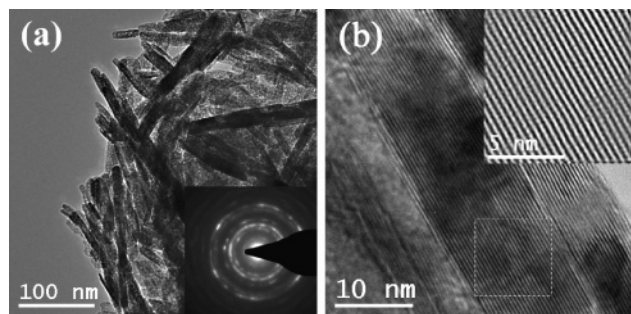


Figure 2. (a) Typical TEM image of CoOOH nanorods with a selected-area electron diffraction pattern; (b) a high-resolution TEM image with individual CoOOH nanorod with IFFT analysis.

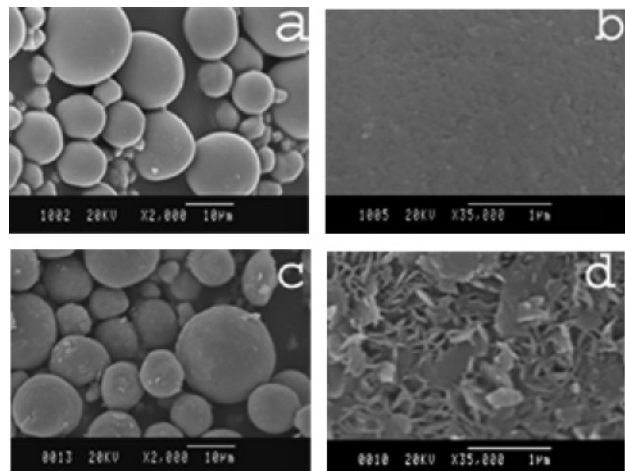


Figure 3. SEM images of (a) uncoated spherical nickel hydroxide particles and (b) magnification of particle (a); (c) coated spherical nickel hydroxide particles and (d) magnification of particle (c).

(003) plane was determined to be 4.405 Å. These parameters are in accord with those of bulk CoOOH ($a = 2.849$ Å and $c = 13.130$ Å, JCPDS 14-0673).

Figure 2a gives a typical TEM image of the sample, illustrating a rodlike morphology with a length of 100–200 nm and diameters of 10–15 nm. The selected-area electron diffraction (SAED) pattern as inserted in Figure 2a exhibits that the nanorods have a polycrystalline structure with a good crystallinity. The high-resolution TEM (HRTEM) images (Figure 2b) show that the planar structure of a single nanorod is in uniform alignment. The calculated interference fringe spacing is about 0.441 nm from the HRTEM image with an inserted IFFT analysis in Figure 2b, which corresponds to the (003) plane of rhombohedral CoOOH and is in good agreement with the value derived from the XRD data.

For the surface modification of nickel hydroxide particles, β -phase spherical nickel hydroxide powders with a particle size of 10–20 μm and a tap density of 2.1 g/mL were added in the above precipitation process of CoOOH. After coating treatments, the product was washed with distilled water to neutral, filtered, and dried at 65 °C. The coating amount was estimated to be 5–7 wt %. The color of nickel hydroxide particles changed to black from green of uncoated samples. The surface morphology of nickel hydroxide particles was studied by scanning electronic microscope (SEM). Figure 3 shows the SEM images of uncoated and coated spherical nickel hydroxide particles. Compared with the uncoated samples, the coated nickel hydroxide particles show the rodlike grain morphology on the surface of nickel hydroxide particles (Figure 3d), which has a length of about 100–300 nm.

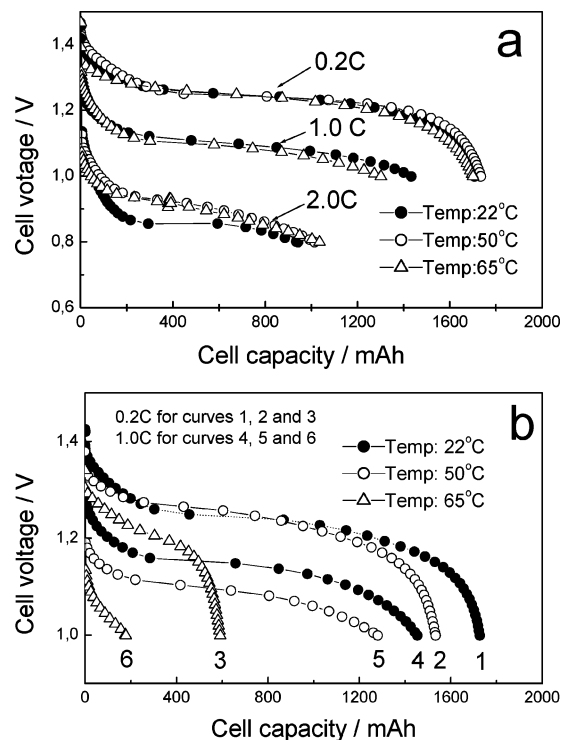


Figure 4. Discharge curves of AA size Ni-MH cells at three different temperatures, 0.2C charge for 6 h and rest for 30 min. (a) The positive is composed of coated nickel hydroxide powders; (b) The positive is composed of uncoated nickel hydroxide powders.

To evaluate its electrochemical properties and applications in the Ni-MH cells, cylindrical AA size Ni-MH cells were assembled by spirally winding positive and negative electrodes along with a 0.12 mm thick polyolefin nonwoven cloth. The positive electrode having a thickness of 0.85 mm was prepared from the coated nickel hydroxide particles. The negative electrode with a thickness of 0.35 mm was composed of 97.5 wt % AB₅-type hydrogen storage alloy, 1.0 wt % black carbon, and 1.5 wt % binder (poly(tetrafluoroethylene)). The electrolyte used was a 7 M KOH solution containing 1 M LiOH. Figure 4a shows the electrochemical performances of the AA size Ni-MH cells. For comparison, the performance of the same size Ni-MH cells, in which the positive was made of 90% uncoated nickel hydroxide, 6% cobalt oxide, 2% Ni powder, and 2% binder materials, was also given in Figure 4b. As seen from Figure 4a, the cell has a capacity of 1700–1800 mAh at a 0.2C rate and can deliver the almost same discharge capacity from 0.2 to 2.0C rates at three temperatures of 22, 50, and 65 °C, respectively. In contrast, the latter Ni-MH cells, where the positive electrode consisted of uncoated nickel hydroxide powders, exhibited poor performance (see Figure 4b). At 65 °C, the cell delivered its capacity of only 600 mAh at 0.2C (curve 3 in Figure 4b) and 180 mAh at 1.0C (curve 6 in Figure 4b), only 35% and 14% capacity of the former Ni-MH cell, respectively. These results indicate that the Ni-MH cell, where the positive electrode was composed of coated nickel hydroxide, can maintain high performance at elevated temperatures.

To further examine the influence of CoOOH nanorods on the charge efficiency, the charge curves of the two kinds of Ni-MH cells at various temperatures were measured and the results are shown in Figure 5. As is seen, the Ni-MH cell composed of the coated nickel hydroxide particles had a relatively flat charge voltage in the first 4 h of charge time, and then the cell voltage started to raise and subsequently reached another flat near to the charge terminate. The quick

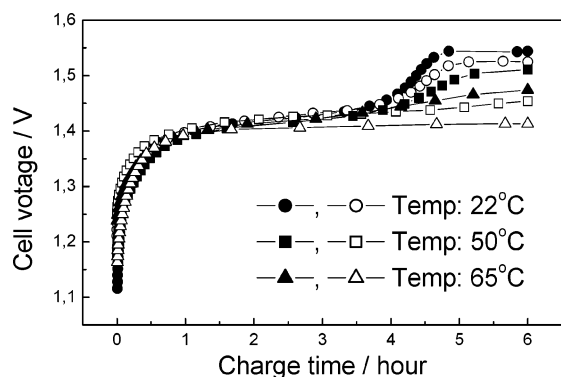


Figure 5. Charge curves of two kinds of AA size Ni-MH cells at a 0.2C rate and three temperatures. ●, ■, ▲ Curves are made of coated nickel hydroxide particles. ○, □, △ Curves are made of uncoated nickel hydroxide particles.

rise of the charge voltage indicated that oxygen gas started evolution on the positive electrode and a lot of oxygen gas would be produced near the charge terminate. The oxygen evolution potential decreased as the operation temperature increased from 22 to 65 °C. By comparison, the Ni-MH cell composed of uncoated nickel hydroxide particles had similar charge curves at temperatures of 22 and 50 °C. However, they had a lower oxygen evolution potential compared to the charge curves of the former Ni-MH cell. This implies that the latter Ni-MH cell had a slightly lower discharge capacity due to the lower charge efficiency at temperature of 50 °C. At 65 °C, the latter Ni-MH cell showed a very flat charge voltage and not such a rise of charge voltage near to the charge terminate, as shown in Figure 5. This indicated that the oxygen gas evolution accompanied with the charge process from the initial stage, leading to low charge efficiency and poor performance (curves 3 and 6 in Figure 4b).

The nanostructural materials generally show different physical and chemical properties compared with their polycrystalline counterparts.²³ It has been reported that the nanosized metal oxides (CoO, CuO, etc.) and nickel hydroxide as electrode materials in lithium ion and NiMH batteries showed superior electrochemical properties.^{12,24–26} The improvements of performance were believed to be relative to enhancement of surface electrochemical reactivity as the particle size decreased.¹² The CoOOH material not only appears to have a higher conductivity but also is capable of increasing oxygen evolution overpotential.²⁷ Due to the high degree of disorder and defects on the surface of nanostructural materials,²⁸ the CoOOH nanorods could have superior surface activities so that they readily capture oxygen species to form a nonstoichiometric $\text{Co}^{3+}_{1-x}\text{Co}^{4+}_x\text{OOH}_{1-x}$ phase²⁹ in the period of charge terminate and depress oxygen evolution. In addition, the mixed-valence cobalt oxides have a unique electronic structure and exhibit higher activities for oxygen diffusion or oxygen transport,³⁰ which facilitates the oxidation of nickel(II) hydroxide to nickel(III) oxyhydroxide. These benefits probably lead to higher charge efficiency of the coated CoOOH nickel hydroxide. Our experiment results (see Figure 5) proved this point, and the possible reaction processes were proposed as above. However, the real working mechanism is still not quite clear at the moment and needs to be further investigated.

In conclusion, CoOOH nanorods were synthesized by means of chemical precipitation with an assistance of oxidation treatments. The CoOOH shows rodlike shapes having a length of about 100–200 nm and diameters of 10–15 nm. The surface modification of nickel hydroxide particles was done through coating the CoOOH nanorods in order to improve the performances of Ni-MH cells at elevated temperatures. It has been demonstrated that the Ni-MH cells have higher charge efficiencies and excellent discharge performance at elevated temperatures, where the positive electrodes were composed of the coated nickel hydroxide.

Acknowledgment. This work is supported by the 973 Program (2002CB211800), Program for New Century Excellent Talents in University, and TNSF (033804411), China.

References and Notes

- (1) Kurmoo, M. *Chem. Mater.* **1999**, *11*, 3370.
- (2) Kurmoo, M.; Kumagai, H.; Hughes, S. M.; Kepert, C. J. *Inorg. Chem.* **2003**, *42*, 6709.
- (3) Feyerherm, R.; Loose, A.; Rabu, P.; Drillon, M. *Solid State Sci.* **2003**, *5*, 321.
- (4) Ji, L.; Lin, J.; Zeng, H. C. *J. Phys. Chem. B* **2000**, *104*, 1783.
- (5) Thormahlen, P.; Skoglundh, M.; Fridell, E.; Andersson, B. *J. Catal.* **1999**, *188*, 300.
- (6) Auschitzky, E.; Boffa, A. B.; White, J. M.; Sahin, T. *J. Catal.* **1990**, *125*, 325.
- (7) Radwan, N. R. E.; Mokhtar, M.; El-Shobaky, G. A. *Appl. Catal. A: General* **2003**, *241*, 77.
- (8) Schmidt-Szalowski, K.; Krawczyk, K.; Petryk, J. *Appl. Catal. A: General* **1998**, *175*, 147.
- (9) Klisurski, D.; Pesheva, I.; Abadzhieva, N.; Mitov, I.; Filkova, D.; Petrov, L. *Appl. Catal.* **1991**, *77*, 55.
- (10) Barbero, C.; Planes, G. A.; Miras, M. C. *Electrochem. Commun.* **2001**, *3*, 113.
- (11) Ookubo, A.; Ooi, K.; Hayashi, H. *Langmuir* **1993**, *9*, 1418.
- (12) Poizot, P.; Laruelle, S.; Grugeon, S.; Dupont, L.; Tarascon, J. M. *Nature* **2000**, *407*, 496.
- (13) Sood, A. K. *J. Appl. Electrochem.* **1986**, *16*, 274.
- (14) Oshitani, M.; Yufu, H.; Takashima, K.; Tsuji, S.; Matsumaru, Y. *J. Electrochem. Soc.* **1989**, *136*, 1590.
- (15) Armstrong, R. D.; Griggs, G. W. D.; Charles, E. A. *J. Appl. Electrochem.* **1988**, *18*, 215.
- (16) Ogasawara, T.; Tokuda, M.; Yano, M.; Fujitani, S. EP 1251574 A2, 2002.
- (17) Oshitani, M.; Watada, M.; Tanaka, T.; Iida, T. *Proc. Electrochem. Soc.* **1994**, 94–27, 303–328 (Hydrogen and Metal Hydride Batteries).
- (18) Onishi, M.; Tanaka, T.; Oshitani, M. JP 10064535 A2, 1998.
- (19) Hong, K.; Lin, Y. M. US Pat 20010012586 A1, 2001.
- (20) Wang, X. Y.; Yan, J.; Yuan, H. T.; Zhou, Z.; Song, D. Y.; Zhang, Y. S.; Zhu, L. G. *J. Power Source*, **1998**, *72*, 221.
- (21) Ding, Y.; Yuan, J.; Wang, Z.; Yong, D.; Sheng, G. B. *J. Power Sources* **1997**, *66*, 55.
- (22) Pralong, V.; Delahaye-Vidal, A.; Beaudoin, B.; Gerand, B.; Tarascon, J. M. *J. Mater. Chem.* **1999**, *9*, 955.
- (23) The special issue “Nanostructured materials”; *Chem. Mater.* **1996**, *8*.
- (24) Gao, X. P.; Lan, Y.; Zhu, H. Y.; Liu, J. W.; Ge, Y. P.; Wu, F.; Song, D. Y. *Electrochem. Solid-State Lett.* **2005**, *8*, A26.
- (25) Reiser, D. E.; Salkind, A. J.; Strutt, P. R.; Xiao, T. D. *J. Power Sources* **1997**, *65*, 231.
- (26) Zhang, Y. S.; Zhou, Z.; Yan, J. *J. Power Sources* **1998**, *75*, 283.
- (27) Wang, X. Y.; Yan, J.; Zhang, Y. S.; Yuan, H. T.; Song, D. Y. *J. Appl. Electrochem.* **1998**, *28*, 1377.
- (28) Penn, R. L.; Stone, A. T.; Veblen, D. R. *J. Phys. Chem. B* **2001**, *105*, 4690.
- (29) Pralong, V.; Delahaye-Vidal, A.; Beaudoin, B.; Leriche, J. B.; Tarascon, J. M. *J. Electrochem. Soc.* **2000**, *147*, 1306.
- (30) Nemudry, A.; Rudolf, P.; Schollhorn, R. *Chem. Mater.* **1996**, *8*, 2232.